

ARTICLE

Empirical model for determining compressive strength using post-installed pull-out test for structural lightweight concrete made with sintered flyash lightweight aggregate

Brijesh Singh^{1,2} | Shamsher Bahadur Singh¹ | Sudhirkumar V. Barai¹ |
P. N. Ojha² | Rohit Kumar²

¹Department of Civil Engineering, Birla Institute of Technology and Science, Pilani, India

²Centre for Construction Development and Research, National Council for Cement and Building Materials, Ballabgarh, India

Correspondence

Brijesh Singh, Department of Civil Engineering, Birla Institute of Technology and Science, Pilani, India.
Email: brijesh.singh@ncbindia.com

Abstract

In recent years, structural lightweight concrete has gained momentum in its use due to its superior properties in terms of dead load reduction, better thermal comfort, improved fire resistance, etc. The use of lightweight aggregates manufactured from industrial bi-products such as flyash presents an alternative to ever-depleting natural aggregates and has been the solution to environmental challenges and a circular economy. With the increase in the use of sintered flyash lightweight aggregate-based concrete (LC-SFA), there is a need to evaluate the applicability of existing empirical equations and models available to predict the on-site strength of concrete using the pull-out method. The pull-out technique for on-site strength estimation has been well researched for normal concrete (NC), but very limited studies have been reported for structural lightweight concrete. This study aimed to develop a model for the determination of on-site compressive strength from 20 to 50 MPa for lightweight concrete (LC) with sintered flyash lightweight aggregate with a high degree of predictability and accuracy using the non-destructive pull-out test, and compare the results with normal weight concrete. The pull-out method adopted in the study has demonstrated that the in-place compressive strength of concrete can be predicted with high accuracy and better repeatability of LC-SFA. The percentage variation in compressive strength predicted by different models varies from -2% to 80%. The proposed model for normal concrete and the model developed by Jensen and ACI for normal concrete gave values somewhat near to the experimental results of LC, however, the variation was more than 15% in the case of ACI, and in the case of Jensen, the values were on the lower side. The study revealed that existing empirical equations available for normal weight concrete to predict the compressive strength on the basis of pull-out force will not be applicable to lightweight concrete, and proposed a model based on a study conducted gives high accuracy and repeatability.

KEYWORDS

compressive strength, lightweight concrete, model, normal weight concrete, pull-out, sintered flyash lightweight aggregate, stress-strain

1 | INTRODUCTION

Concrete is a comparatively bulky building material in terms of its weight, and researchers in the past have developed alternative concrete, such as lightweight concrete, porous concrete, pervious concrete, etc., to reduce its weight without impacting its other properties. Among this, the structural lightweight concrete presents several advantages over normal weight concrete in terms of improved thermal performance, superior fire resistance, and reduced dead load resulting in lower cost of formwork, transportation, labor, etc., with major benefits observed in the precast concrete industry.¹ One of the ways to produce manufactured lightweight aggregate for the production of lightweight concrete is by utilizing flyash as the main raw material through the sintering process. The scarcity of natural aggregates presents a need to use alternative man-made aggregates, which in one way or the other tackle the problems of environmental issues and promote circular economy and sustainable construction. Looking into the large legacy stock of flyash available in India, the use of sintered flyash lightweight aggregate in concrete construction is getting more and more attention and adoption in construction.^{2,3} With the increase in use of structural lightweight concrete, there is a need to examine the non-destructive testing (NDT) methods used in the evaluation of on-site strength of new and old concrete structures. The strength of concrete determined on concrete cube specimens prepared, compacted, and cured under laboratory conditions is different from the actual built structure. The difference in determined strength also depends on the shape and size of the concrete specimen, and the accuracy of the test method is influenced by these factors. For on-site strength determination, different NDT methods have been adopted in the past, and one of the methods developed for quick assessment of compressive strength is a pull-out test. Numerous studies have been carried out using this method for normal-weight concrete in general, with limited studies being available for lightweight concrete. Researchers such as Skramtjæw,⁴ Rutenbeck,⁵ Kierkegaard,⁶ Malhotra,⁷ Richards,⁸ Stone and Carino,⁹ Collins and Roper,¹⁰ etc. have demonstrated the applicability of the pull-out method for the determination of on-site strength of concrete. In the past, different innovative methods have been developed to assess the on-site strength of concrete, such as the arc pressure testing (APT) method,¹¹ double shear testing method (DSTM),¹² hammer pendulum test method,¹³ and modified pull-out testing method (MPTM).¹⁴ The test results in the APT method highlighted that it is suitable for on-site compressive strength determination of concrete in the case of prefabricated structures and beam-column joints of structures

with dense reinforcement. The APT method, compared to other on-site strength determination test methods, showed higher accuracy with minimum damage to the structure.¹¹ The double shear test method involves a load being exerted through the DSTM apparatus on the double shear face of the concrete core to produce pure shear stress for obtaining the shear strength of the concrete core.¹² The repeatability and reliability of DSTM were reported by Yang et al.¹² to be greater compared to other on-site strength compressive strength measurement techniques, such as the rebound hammer and pull-off test method. The relationship between the depth of penetration versus compressive strength using the hammer pendulum test concluded that the developed method is an alternative compression test method for masonry mortar with a minimum level of preparation, high accuracy, and better repeatability.¹³ The MPTM test method was introduced by Yang et al.,¹⁴ which also involved an improvement in the classical method through the use of a cup-shaped loading probe in order to ensure that pure axial load is applied in the tensile strength measurement. The MPTM Test findings have indicated that results do not depend upon the test direction, diameter, and depth of core as well as aggregate size. This method has been reported to be more repeatable and reliable compared to the conventional pull-off test method.¹⁴ The pull-out method measures the force needed to extract an inserted metal having an enlarged head from a concrete member. The pull-out force is given to the insert by a hydraulic jack counterbalanced by the ring in such a way that the insert extracts concrete in a conical shape, and the dimension of the cone depends upon the size and geometry of the experimental setup. Under this scenario, the ultimate limit state situation is obtained, consisting of a state of combined compressive and shear stress, making the test exceptionally reliable.^{12,15} The study by Kierkegaard⁶ highlighted that an increase in ultimate load happens because of the state of stress internally within the region of failure. The failure surface obtained from the pull-out test method is similar to the failure surface of concrete slabs in punching conditions when the bearing ring is of a large radius. The literature survey indicates that there are studies and models available on the pull-out method for the determination of on-site strength of normal weight concrete, but very limited studies and models are available on the pull-out method of lightweight concrete. The present study aims to experimentally evaluate the compressive strength using the pull-out method for LC-SFA for a wide range of compressive strengths from 20 to 50 MPa. The theoretical boundary condition of the pull-out test considered in this study relates to concrete being subjected to compression between the counter-pressure ring and expanded ring,

wherein concrete is assumed to be homogenous, linear elastic, infinite half-space with radial symmetry. The compressive strength of concrete is directly related to the pull-out force needed to dislodge the concrete frustum. In the test, the steel disk has been assumed to be perfectly bonded with the concrete until failure. The top surface of the concrete subjected to pull-out force has been assumed to be free from external stresses. The pull-out test involved drilling a hole into concrete to a specific depth and diameter (the hole diameter was 18.4 mm and the expanded insert diameter was 25 mm). During the test, concentric load is applied as a pulling force to the ring, where the applied force is pointed towards the middle portion of the recess. The pull-out test was complete at the point when the conic frustum of concrete is dislodged. The heterogeneity of concrete is not considered, and the test assumes radial symmetry. The study also presents a comparison of the model developed based on experimental data for the prediction of on-site strength of LC-SFA with existing models for lightweight concrete.

2 | MATERIALS

In this study, lightweight concrete was produced using Ordinary Portland Cement (OPC) 43 Grade conforming to IS 269, sintered flyash lightweight aggregate (SFA), silica fume, a polycarboxylic ether-based superplasticizer conforming to IS 9103, and fine aggregates conforming to Zone II requirements of IS 383:2016. The SFA, used as coarse aggregate, is brown with a black core, as shown in Figure 1, and its microstructure is illustrated in Figure 2. Two size fractions of SFA, 8–16 mm and 4–8 mm, were utilized. The mechanical properties of SFA are listed in Table 1, and the chemical composition of SFA and OPC43 Grade cement is provided in Table 2.

The X-ray diffraction (XRD) curve of sintered flyash lightweight aggregate is shown in Figure 3. The results indicate the presence of different crystalline phases such as quartz, mullite, muscovite, and albite. The hump in XRD curve is characteristic of presence of glassy phase. These sintered aggregates produced through the sintering method have shown a quartz peak with a mild peak of mullite. The abundance and type of crystalline phases are dependent on the sintering temperature and composition of flyash. The SFA under study comprises of class F flyash (90%–92%), bentonite clay as a binder (1%–1.5%), and coal (7%–8%). The sintering temperature for this aggregate has been 1200°C. The higher sintering temperatures can lead to the formation of a specific phase, and transformation happens to already existing phases. XRD study has indicated that with an increase in treatment temperature on aggregate, a reduction in the quartz peak

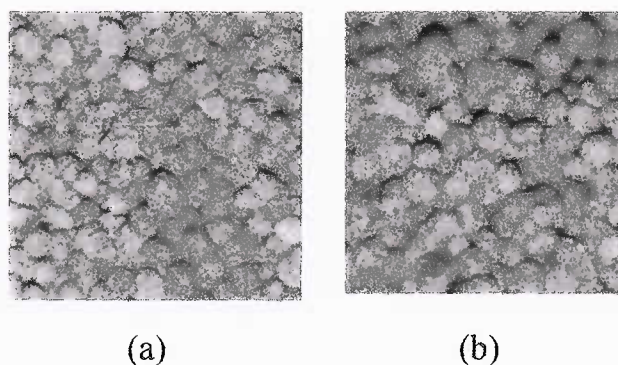


FIGURE 1 (a) Sintered flyash aggregate, 4–8 mm. (b) Sintered flyash aggregate, 8–16 mm.

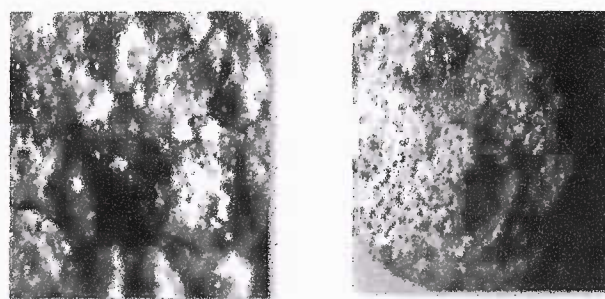


FIGURE 2 Microstructure of sintered flyash lightweight aggregate (10 μm and 1.5×).

occurs, and there is a mild increase in the mullite peak.^{1,2,16} For the quartz phase, possible crystallization can come into play during the cooling stage, but under no circumstances it would be able to counteract the lattice decomposition happening in the pre-sintering phase. The mullite formed during the sintering phase contributes to the strength as well as durability of lightweight aggregate. The combined grading of the coarse aggregate conforms to the IS: 9142-2018¹⁷ and is shown in Figure 4.

3 | MIX DESIGN

Sintered fly ash lightweight aggregates are highly porous and exhibit a significantly higher water absorption rate (about 18%) compared to conventional aggregates, which absorb about 1.5%. This characteristic necessitates a distinct mix design method for lightweight concrete, as traditional methods used for normal aggregate concrete are inadequate. Adding extra water equivalent to the aggregate's absorption capacity directly into the mix leads to segregation and reduction in the water-to-cement (w/c) ratio, ultimately compromising the concrete's mechanical properties.^{18–20} The direct correction for water does not

TABLE 1 Mechanical properties of SFA used in the study.

Fraction	LWA designation	Specific gravity	Water absorption at 24 h (%)	Loose bulk density (kg/m ³)	Crushing strength (N/mm ²)	10% fines (ton)
4–8 mm	LWA-I	1.47	17.50	813	8.80	-
8–16 mm	LWA-II	1.49	17.93	849	7.70	3.60

TABLE 2 Chemical composition of SFA and OPC cement.

Component	CaO (%)	SiO ₂ (%)	Al ₂ O ₃ (%)	Fe ₂ O ₃ (%)	SO ₃ (%)	MgO (%)	Na ₂ O equivalent (%)	Loss of ignition
SFA	2.45	62.50	25.85	4.19	0.29	0.53	0.77	1.48
Cement OPC 43 grade	59.60	21.22	7.19	4.25	2.50	1.90	1.05	1.94

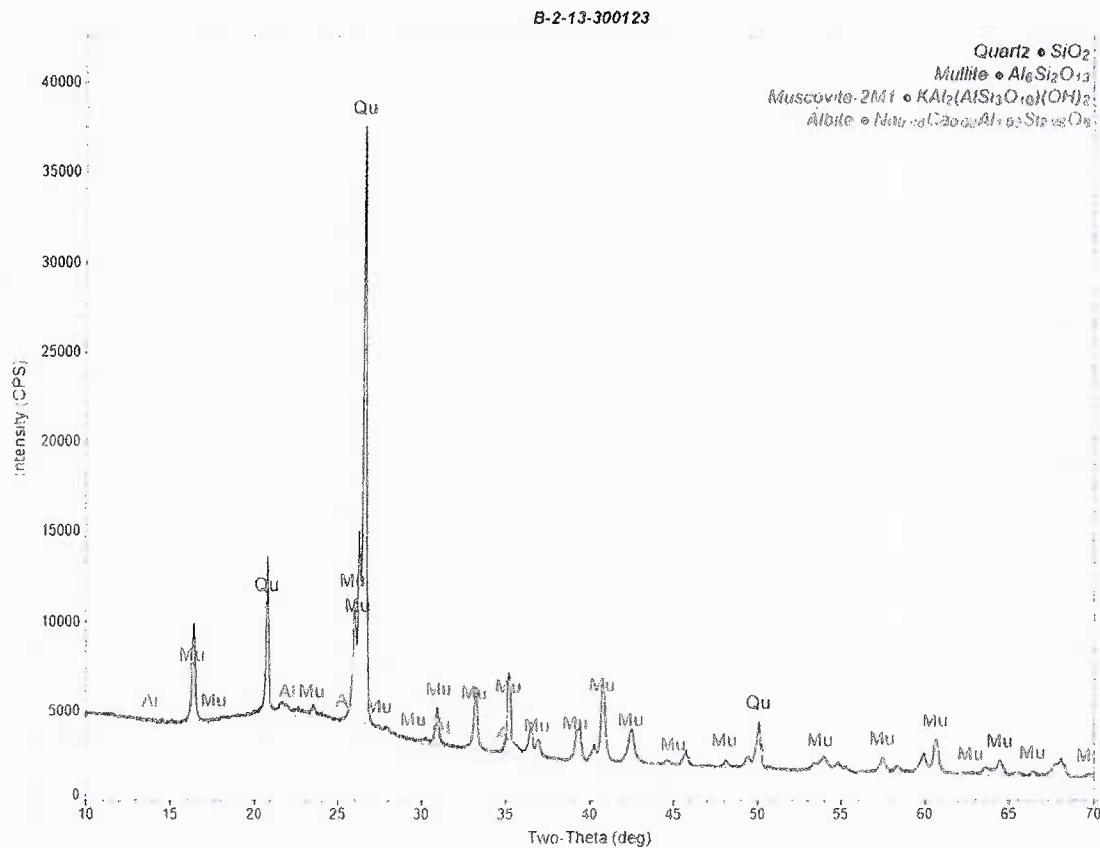


FIGURE 3 X-ray diffraction curves of sintered flyash lightweight aggregates.

account for the influence of cement paste, which plays an important role in the determination of the water absorption capacity of lightweight aggregate concrete. To address these challenges, Singh et al.¹⁸ water absorption curves incorporate the effect of cement paste for various w/c ratios along with IS: 10262-2019,²¹ which is used for mix design. Initially, 75% of the water is added to the dry mix of materials, and mixing is carried out for

2–3 minutes to achieve initial homogeneity. Subsequently, the remaining water, along with the admixture, is added and mixed for an additional mixing period to ensure consistency and workability. The obtained slump was 75–100 mm. The concrete mix design is shown in Table 3 (panels a and b) for a w/c ratio of 0.3 to 0.7 for both lightweight and normal weight concrete, respectively. The prepared concrete mix is then compacted into

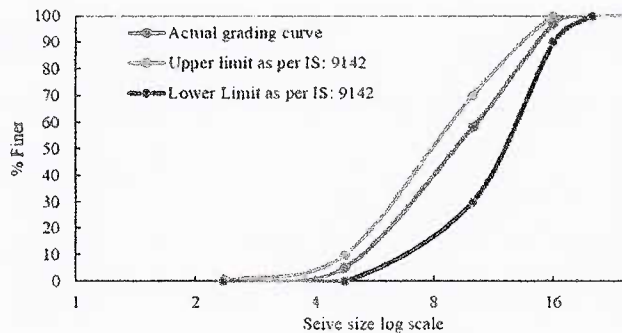


FIGURE 4 Combined grading of the sintered flyash lightweight aggregate used in the study as per IS 9142,¹⁷ upper and lower limits.

the molds of the cube and cylinder in three layers. The demolding process was carefully carried out after 24 h, ensuring the specimens retained their shape without damage. Once demolded, the concrete cubes were transferred to a curing environment that adhered to controlled laboratory conditions, with a maintained temperature of $27^{\circ}\text{C} \pm 2^{\circ}\text{C}$ and relative humidity of 65% or more.

4 | DETAILS OF THE SPECIMEN

The concrete cube and cylinder specimens of strength range from 20 to 50 MPa were prepared for carrying out the pull-out test and measuring compressive strength in the laboratory, while the cylindrical sample was cast to find out compressive strength and carry out the stress-strain test. Concrete specimen sizes prepared for the tests are outlined in Table 4. The 150 mm size cubes and cylindrical specimens with a 150 mm diameter and 300 mm height have been used to evaluate the compressive strength as per IS: 516.²² The pull-out testing was conducted as per ASTM C900.²³ The prepared test specimens are shown in Figure 5.

5 | CAPO-TEST PRINCIPLE

The on-site compressive strength of the existing structure is measured by NDT tests. The outlines and procedure for the use of the CAPO (cut and pull-out) test for the determination of compressive strength are mentioned in the ASTM C900,²³ BS 1881-207,²⁴ and EN 12504-3.²⁵ The basis of the pull-out test is force needed for the complete failure of the specimen is proportional to the concrete's compressive strength measured by a standard cube or cylinder.²⁴ The primary instrument used in the test is a hydraulic pull machine having gauge ranges from 0 to 100 kN.²⁵ The standard rate of loading for a pull-out test

involves applying a force at a consistent rate, measured in millimeters per minute or Newtons per second. A loading rate of 0.5 ± 0.2 kN/s for 25 mm diameter inserts was used in the present study.²⁴ ASTM C900 insists on the importance of a controlled loading rate and mentions the need for a loading apparatus with sufficient capacity to provide the decided loading rate.²³ This machine is designed to apply a controlled pull-out force to the split ring inserted into the concrete. The hydraulic pull machine has precise control and measurement, with an internal resolution of 0.01 kN. The rate of loading during the test has been applied gradually and without shock to avoid premature failure or inaccuracy in the obtained results. To determine the compressive strength of hardened concrete using the pull-out test, the proper selection of the test location is crucial. The selected location must be free from reinforcement bars within the failure zone. The geometry of the test depends on the nominal maximum size of the aggregate. Based on this size, the diameter, d_2 , of the expandable insert head is chosen, which should be at least two-thirds of the nominal maximum aggregate size. The shaft diameter, d_s , should not be more than 0.6 times the d_2 . The test begins by drilling a core hole with a diameter d_1 and a depth of approximately $2.5d_1$, normal to the concrete surface, using a diamond-studded core bit. The top surface of the drilled hole is then smoothed, and a recessed groove with a diameter of d_2 is created at a depth equal to d_2 using a diamond-impregnated grinding wheel. An expandable insert, attached to an expansion tool, is placed into the hole, ensuring it fits into the recess. When pulled during the test, the insert expands and interacts with the concrete.

The complete test procedure is shown in Figure 6 as per the ASTM C900. Figure 6a shows the drilled hole and recess after smoothing the top surface. Figure 6b shows the expandable insert in the hole. Figure 6c shows the recess occupied by an expandable insert. Figure 6d shows the complete pull-out setup with the placement of a counter-pressure ring (bearing ring) on the center of the surface. The counter-pressure ring, placed centrally on the surface, has an internal diameter of approximately 2.0–2.4 times the diameter of the insert head d_2 . The surface beneath the counter-pressure ring must be smooth to ensure uniform pressure distribution. Finally, the hydraulic pull machine applies a load until failure occurs in the concrete between the counter-pressure ring and the expanded insert. In the experiment conducted, the hole diameter d_1 was 18.4 mm, the expanded insert diameter d_2 was 25 mm, and the counter-pressure ring's internal diameter d_3 was 55 mm. Figure 7a,b show the generalized dimensions and a cross-sectional view of the instrument used, based on the instrumentation manual.

TABLE 3 Concrete mix design details of lightweight concrete and normal weight concrete.

Panel a: Lightweight concrete

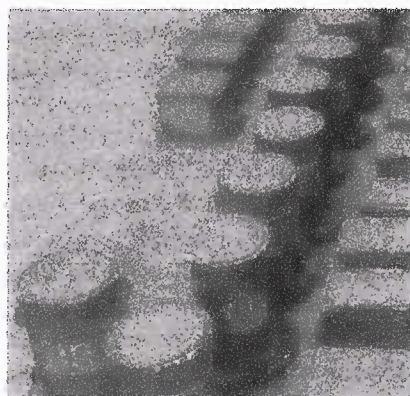
w/c	OPC + silica fume (kg/m ³)	Total water		Aggregate (kg/m ³)			Admixture (kg/m ³)	Compressive strength (MPa)		Density (kg/m ³)	
		Mixing water	Extra water	Coarse				Strength	COV	Density	COV
				Fine	8–16 mm	4–8 mm					
0.7	245 (245 + 0)	170	103	816	383	252	0.10	19.16	6.1	1725	4.3
0.6	285 (271 + 14)	170	96	764	390	256	1.14	23.66	5.2	1743	3.6
0.5	340 (316 + 24)	170	90	708	393	258	2.00	35.66	5.6	1795	3.4
0.4	425 (382 + 43)	170	84	646	390	256	2.60	43.37	3.2	1840	2.6
0.3	566 (481 + 85)	170	64	573	377	248	3.80	57.66	3.5	1880	3.3

Panel b: Normal weight concrete

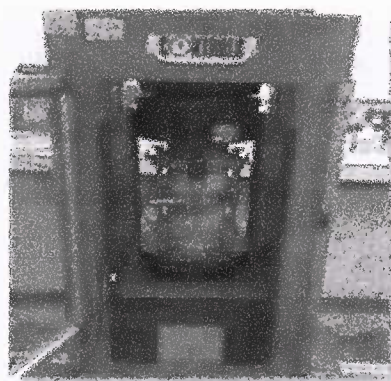
			Aggregate (kg/m ³)			Admixture (kg/m ³)	Compressive strength (MPa)		Density (kg/m ³)	
w/c	OPC + silica fume (kg/m ³)	Water content (kg/m ³)	Fine	Coarse			Strength	COV	Density	COV
				20 mm	10 mm					
0.7	245 (245 + 0)	170	705	805	540	0.20	23.50	3.77	2178	4.4
0.6	285 (271 + 14)	170	690	795	520	0.60	30.50	3.01	2191	3.3
0.5	340 (316 + 24)	170	660	775	516	0.50	43.35	5.27	2224	4.1
0.4	425 (382 + 43)	170	580	775	515	0.80	55.72	3.71	2265	3.7
0.3	566 (481 + 85)	170	493	742	495	1.00	62.85	3.24	2314	2.9

TABLE 4 Specimen dimensions for evaluating compressive strength, pull-out strength and stress-strain.

S. no.	Type of sample	Sample size (mm)	Parameters evaluated
1	Cubes	150 × 150 × 150	Compressive strength and pull-out test
2	Cylinders	150 in diameter and 300 in height	Compressive strength and stress-strain



(a)



(b)

FIGURE 5 (a) Concrete beams in molds, cubes, and cylinders. (b) Test setup for stress-strain behavior of concrete under compression.

Figure 8a,b depicts the CAPO test equipment and its use on a concrete specimen.

The failure mechanism during the test is divided into three stages. The first stage, initial crack formation

during the application of the initial pull-out force, a tensile crack initiates from the top of the expandable insert. This crack length ranges from 15 to 20 mm from the expandable insert head at 30%–40% of the ultimate load.

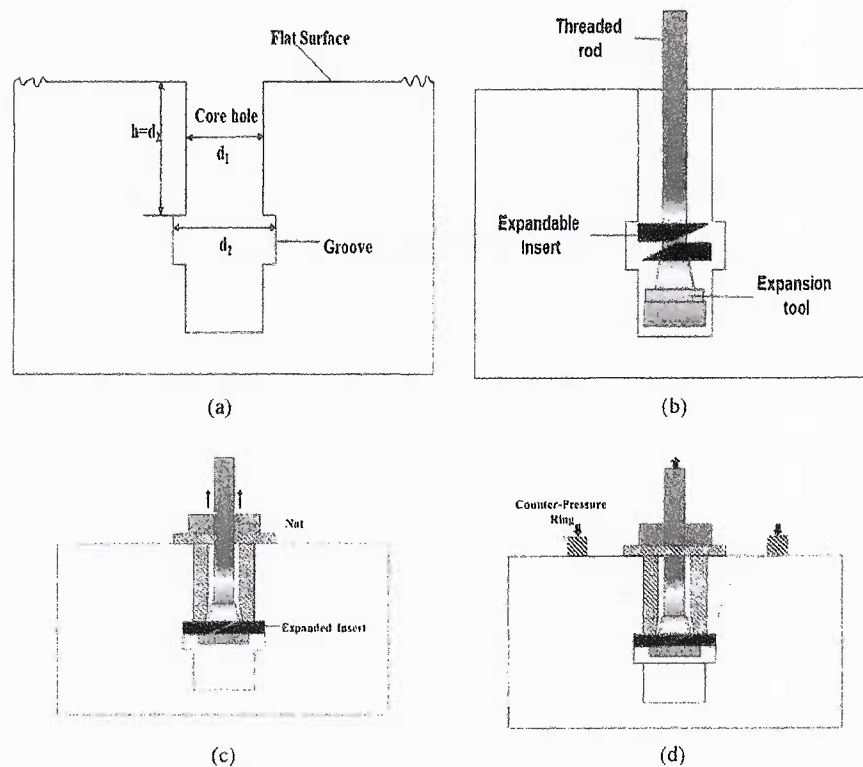


FIGURE 6 (a) Core hole with recess groove with smooth top surface. (b) Expandable insert with expansion tool. (c) Expanded insert. (d) Application of load during test.

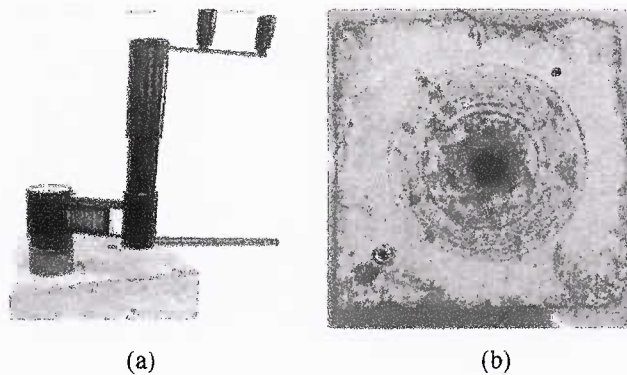
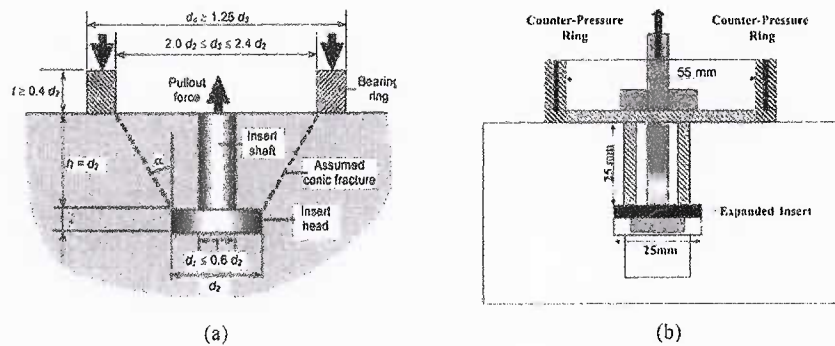
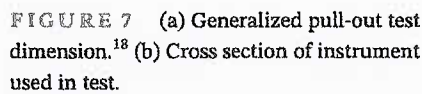


FIGURE 8 (a) Instrumentation for pull-out. (b) Pull-out conducted sample.

This tensile crack is shown in Figure 9a. As the pull-out force increases further, the crack occurs due to compression between the counter pressure and the expandable insert. This compression creates a strut-like mechanism, causing micro-cracks within the concrete similar to those observed in a uniaxial compression test. This causes the compression crack of the second stage, which is shown in Figure 9b. Micro-crack at this stage simulates uniaxial compression testing in the laboratory, which directly correlates with the concrete's compressive strength. In the third stage, when the load applied during a pull-out test reaches its maximum value, the concrete undergoes a third stage of rupture. At this point, a crack forms due to the combined effects of tensile and shear stresses. This

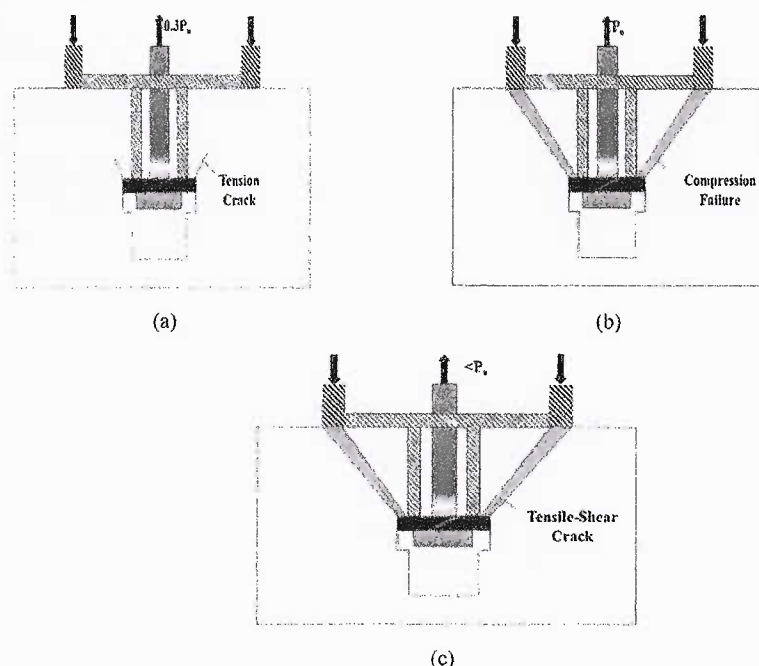


FIGURE 9 (a) Tension crack. (b) Compression crack with formation of micro-crack. (c) Tensile-shear crack.

crack extends from the outer edge of the insert head (the part embedded in the concrete) to the inner edge of the counter-pressure ring (the part that applies the pulling force), creating complete detachment from the parent concrete.^{16,25–34} Figure 9c shows the tensile-shear crack.

The study in the literature on lightweight concrete made with SFA is scant when it comes to models available for on-site determination of concrete using the pull-out test. The sintered flyash lightweight aggregate presents typical microstructural and mechanical characteristics because of the energy intensive and thermally treated sintering process. In comparison to expanded lightweight aggregates or cold-bonded lightweight aggregates, sintered flyash aggregates have exhibited a ceramic-type matrix during the high-temperature sintering method, resulting in an aggregate with high porosity and lower intrinsic crushing strength compared to conventional natural aggregates. These specific properties directly impact the interfacial transition zone (ITZ) and fracture behavior, which are distinctly different from conventional lightweight concretes.^{2,3} Past studies have focused on the mix design or compressive strength of SFA-based lightweight concrete. Now, with an increase in the use of LC-SFA, there is a need to evaluate the applicability of existing empirical and analytical equations and models available to predict the on-site strength of concrete using the pull-out method and develop new models for accurate prediction for LC-SFA. The developed model will provide a reasonably accurate estimation of compressive strength using the pull-out

test, as the conventional compressive strength tests are labor-intensive and require large specimens that are not ideal for on-site quality control. The CAPO test is a simpler and comparatively less destructive method for obtaining the concrete compressive strength value.

6 | RESULTS AND DISCUSSIONS

6.1 | Correlation of pull-out load to cylinder compressive strength

The study aimed at developing a model for the determination of on-site compressive strength of LC-SFA with better predictability and accuracy using the non-destructive pull-out test on more than 70+ samples at 28-day age. The obtained result of the pull-out load was used to find out the correlation between actual cylinder compressive strength vs. pull-out load. The pull-out test, particularly for lightweight concrete, immediately in wet condition, leads to difficulties in achieving a reliable bond for moist cured concrete samples without a sufficient period of drying because the lightweight aggregate's water absorption is higher compared to normal concrete. The results reported are on surface dry concrete with at least 24 h of drying before the test. In the dry state, edges in the case of both lightweight and normal weight aggregates can engage with the cut or interfacial separation, and this situation dictates the failure mode. On the other hand, when the aggregate has moisture, the water

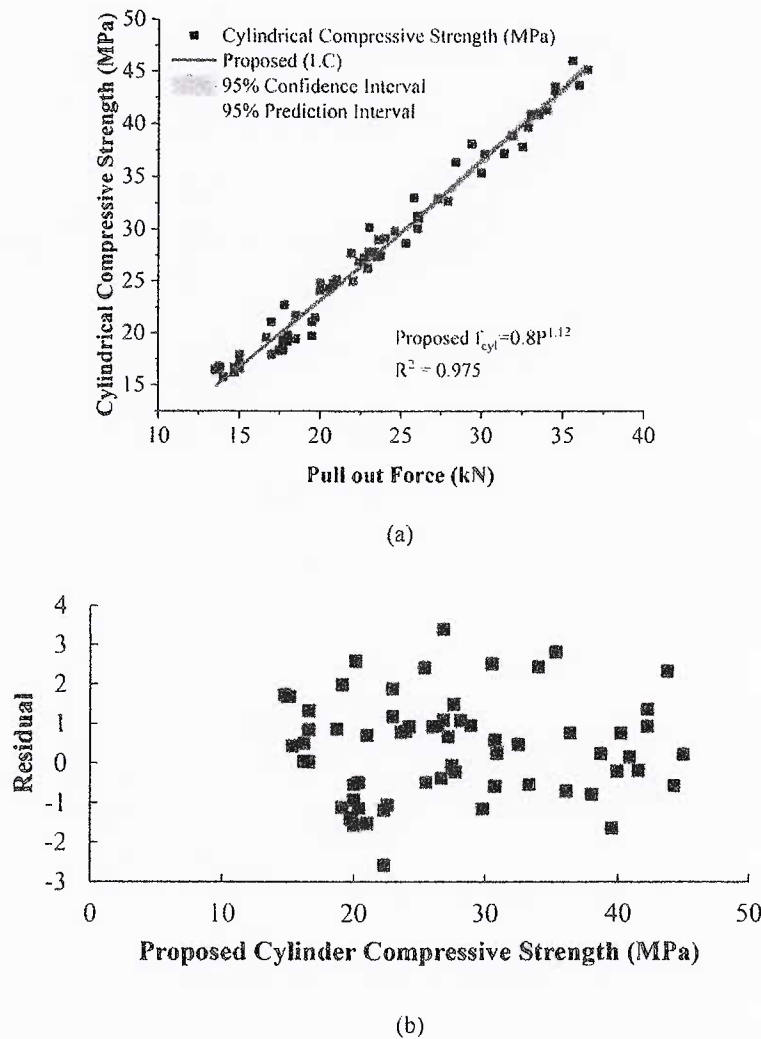


FIGURE 10 (a) Correlation of pull-out load to cylinder compressive strength for LC-SFA. (b) Residual error showing the difference between the observed and predicted compressive strength values against the predicted strength for lightweight concrete.

present decreases the frictional force as the lubricating effect of water makes it difficult to generate the required frictional resistance to start a cut failure. The moisture availability in aggregate weakens the interlock between the aggregate and subsequently decreases the pull-out force required to dislodge the concrete specimen. The SFA in the present study is brought to a dry state condition to decrease the variation in pull-out results.

The interfacial transition zone (ITZ) in the case of LC-SFA is denser compared to normal weight concrete as reported in past studies.^{1–3} The ITZ is denser due to phenomena called internal curing, and reactive surfaces also contribute to prolonged hydration. This leads to the refinement of the microstructure wherein the paste penetrates the porous lightweight aggregates and improves the mechanical interlocking. Due to improved ITZ, the initial bond strength improves in lightweight concrete with sintered flyash lightweight aggregate, but porous

characteristics of lightweight aggregate create the ITZ as a conduit of crack formation once the critical stress level is attained. The porous aggregate, due to improvement in ITZ, improves stress transfer of loads, but inherent characteristics of aggregates in terms of discontinuities create preferred paths for initiation of cracks under the high level of tensile stresses, particularly in the pull-out case. The shift from a peak load to failure is influenced by ITZ quality and the presence in this zone. Since the ITZ is superior in LC-SFA, the load transfer is uniform, leading to a shift in mode of failure from initial adhesive bonding to a mixed failure where micro-cracks start propagating into both the ITZ as well as cement paste, with relatively high energy needed to attain ultimate failure.

The actual cylindrical compressive strength versus pull-out force plot is shown in Figure 10a, and its residual plot is given in Figure 10b for lightweight concrete. Similarly, for normal-weight concrete, it is shown in

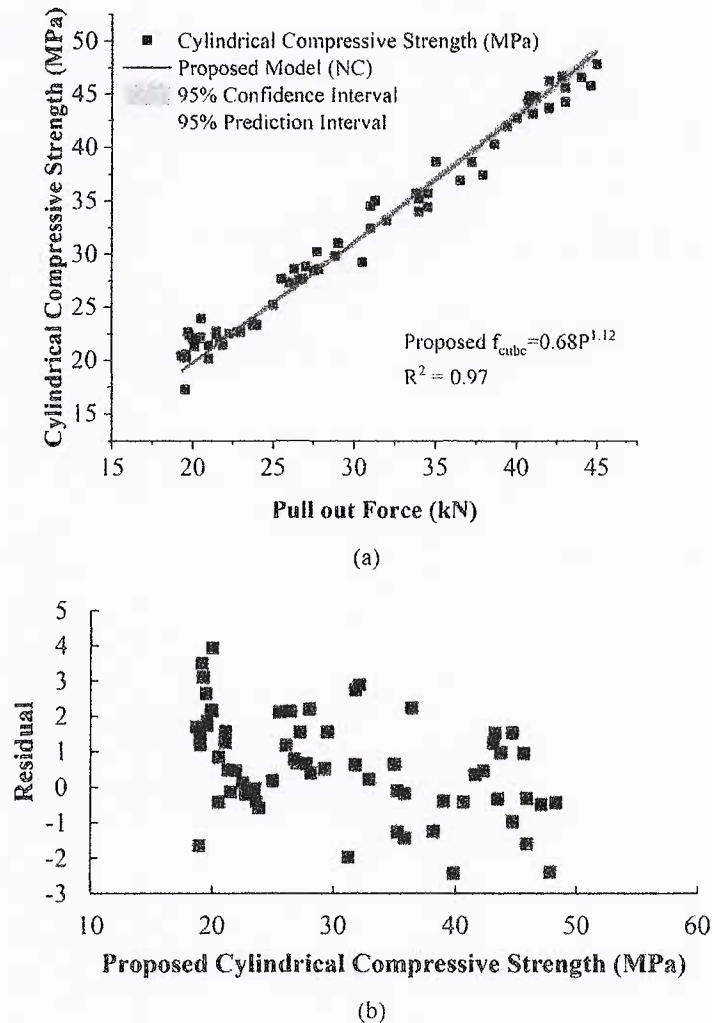


FIGURE 11 (a) Correlation of pull-out load to cylinder compressive strength for normal concrete. (b) Residual error showing the difference between the observed and predicted compressive strength values against the predicted strength for normal concrete.

Figure 11a,b. The fitting process using regression indicated the correlation coefficient (R^2) = 0.97 between pull-out force and compressive strength, indicating a very high level of correlation. From the regression analysis, 95% confidence intervals (CI) and prediction intervals (PI) were calculated. The CI quantifies the uncertainty in estimating the mean compressive strength for a given pull-out load, while the PI accounts for variability in individual observations. Figures 10a and 11a represent the predicted compressive strength, corresponding confidence, and prediction intervals for select values of pull-out load. The narrow CI and reasonable width of PI indicate that the developed model is statistically robust and suitable for practical applications. This demonstrates the fact that pull-out tests can be adopted for on-site compressive strength with a high degree of accuracy. The residual plot was generated by plotting the difference between the observed and predicted compressive strength values against the predicted strength. The residuals appear to be randomly scattered around zero with no

apparent pattern. The residual plot shows values between -2 and 3 MPa, indicating the compatibility of the proposed model. The formula used by the ACI guidelines relates the pull-out force (P) to the compressive strength (f_c) through a calibration factor. The general representation of the formula by ACI is expressed as Equation 1.

$$f_c = k \cdot P^n \quad (1)$$

where f_c is compressive strength of concrete; P is pull-out force measured in the CAPO test; k is calibration constant specific to the concrete type and testing conditions; and n is exponent that correlates pull-out force to compressive strength, determined by empirical testing.

To develop a similar expression in line with the ACI empirical equation, Equation 2 is obtained through non-linear regression analysis for the sintered flyash lightweight aggregate-based concrete, and Equation 3 is proposed for normal weight concrete (NC). Both proposed Equations 2 and 3 show a high correlation coefficient (R^2) of 0.97.

$$\text{Proposed } f_{\text{cyl}} \text{ for lightweight concrete (MPa)} = 0.80 \cdot P^{1.12} \quad (2)$$

$$\text{Proposed } f_{\text{cyl}} \text{ for normal weight concrete (MPa)} = 0.68 \cdot P^{1.12} \quad (3)$$

Figure 12 compares the proposed model (Equation 2) for sintered fly ash aggregate-based lightweight concrete

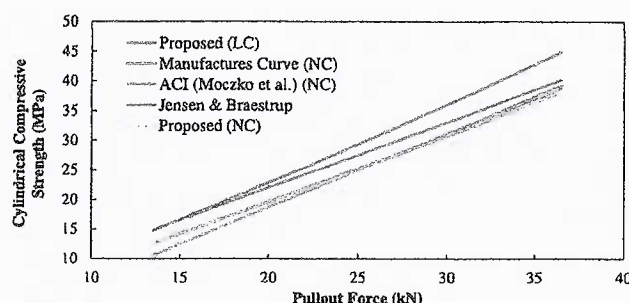
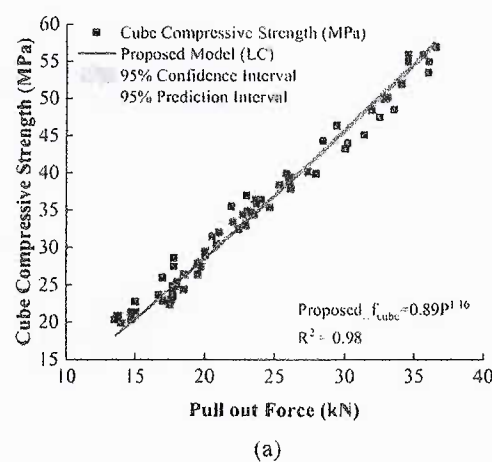
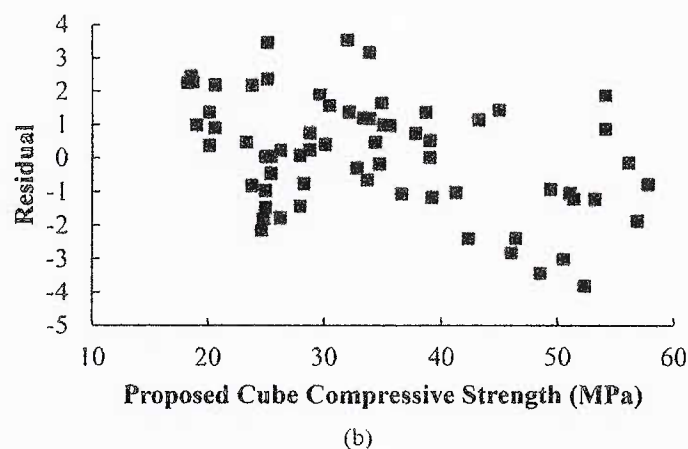


FIGURE 12 Comparison of pull-out load to cylinder compressive strength between the proposed model and other models.

with the proposed model (Equation 3) of normal-weight concrete (NC) and other established models. These include the manufacturer's curve, the ACI-228¹⁵ model, and the Jensen et al.³¹ models for normal-weight concrete (NC), as well as the Krenchel et al.³⁰ model for lightweight concrete (LC). Figure 12 shows that as the pull-out load increases, the compressive strength also increases for both normal and lightweight concrete. For normal-weight concrete, the presence of higher density and strong normal aggregates surrounding the paste provides resistance to failure in the compression zone between the expandable insert and counter-pressure ring of pull-out equipment. Also, it can be inferred that for a given compressive strength, lightweight concrete shows less pull-out force as compared to normal-weight concrete. The difference in test results of compressive strength corresponding the pull-out load obtained experimentally to existing models arises due to the reason that existing models fail to take into account for the lower crushing strength and brittleness of sintered flyash lightweight aggregate and its unique through-aggregate fracture failure mode compared to normal weight aggregates where the normal aggregate avoids through aggregate



(a)



(b)

FIGURE 13 (a) Correlation of pull-out load to cube compressive strength for LC-SFA. (b) Residual error showing the difference between the observed and predicted compressive strength values against the predicted strength for lightweight concrete.

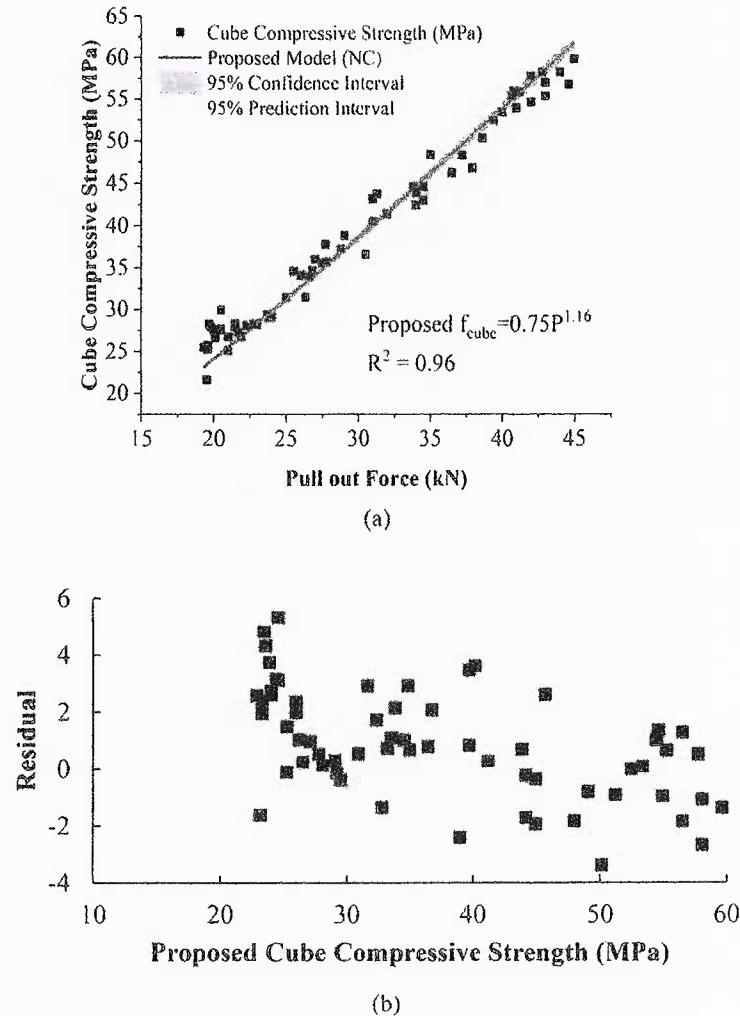


FIGURE 14 (a) Correlation of pull-out load to cube compressive strength for normal concrete. (b) Residual error showing the difference between the observed and predicted compressive strength values against the predicted strength for normal concrete.

fracture mode of failure by resisting the applied pullout load. The localized bond resistance measured through cut and pull-out CAPO tests in the case of lightweight aggregate is not covered in existing models, where global compressive loading and the weak aggregate phase dictate the overall mode of failure.

This difference can be attributed to the combined effects of density and aggregate properties, microstructure differences, brittleness, and failure mechanisms of the concrete. The reduction in pull-out force for lightweight concrete for a given strength level is mainly due to the absence of interlocking between the aggregate, contributing to the failure. The failure mode consists of either vertebral or vertebral-based bond failure. The vertebral failure mode happens during the loading, wherein end displacement at the loading side increases due to an increase in pull-out force, and some increase in displacement is also noticed for a short period during a decrease

in pull-out force. The vertebral failure of the concrete specimen in the pull-out test approximately resembles a frustum of a cone. The radial cracks also get generated during the application of pull-out force on the surface extending outwards to around 30–35 mm from the supporting base. The vertebral-based bond failure is found under the loaded condition. The characteristics of the test surface have a very small influence on modes of failure under the pull-out test, and the most common mode of failure noted is vertebral failure mode.

6.2 | Comparison of pull-out load to cube compressive strength between the proposed model and other models

The pull-out load is correlated with the cube compressive strength, as illustrated in Figures 13 and 14, and its

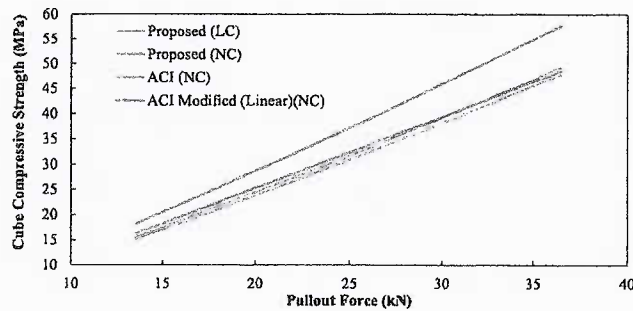


FIGURE 15 Comparison of pull-out load to cube compressive strength between proposed and other models.

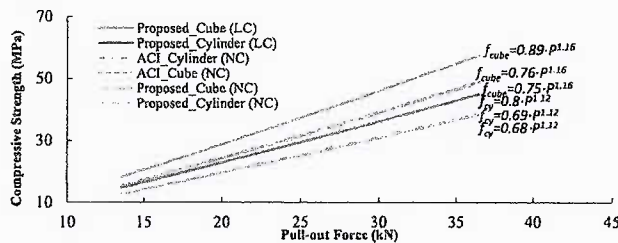


FIGURE 16 Proposed correlation for lightweight concrete.

relationship is represented by the proposed model, as shown in Figure 13a and its residual in Figure 13b for lightweight concrete. Similarly, for normal-weight concrete in Figure 14a,b.

To keep the equation similar to the proposed model for cylindrical compressive strength and ACI-228, Equation 4 is developed through non-linear regression analysis and proposed for the sintered flyash lightweight aggregate-based concrete, and Equation 5 is developed through non-linear regression analysis and proposed for normal-weight concrete (NC). Both proposed Equations 4 and 5 show a high correlation coefficient (R^2) of 0.97, indicating excellent agreement between the predicted compressive strength and the measured values. From the regression analysis, 95% confidence intervals (CI) and prediction intervals (PI) were calculated. The CI quantifies the uncertainty in estimating the mean compressive strength for a given pull-out load, while the PI accounts for variability in individual observations. Figures 13a and 14a represent the predicted compressive strength, corresponding confidence, and prediction intervals for select values of pull-out load. The narrow CI and reasonable width of PI indicate that the developed model is statistically robust and suitable for practical applications. This demonstrates the fact that pull-out tests can be adopted for on-site compressive strength with a high degree of accuracy. The residual plot was generated by plotting the difference between the observed and predicted compressive strength values against the predicted strength. The

residuals appear to be randomly scattered around zero with no apparent pattern. The residual plot of the major portion shows values between -2 and 4 MPa, indicating the compatibility of the proposed model.

$$\text{Proposed } f_{\text{cube}} \text{ for lightweight concrete} = 0.89 \cdot P^{1.16} \quad (4)$$

$$\text{Proposed } f_{\text{cube}} \text{ for normal weight concrete} = 0.75 \cdot P^{1.16} \quad (5)$$

Figure 15 in the comparison of the proposed model (Equation 4) of sintered flyash aggregate-based lightweight concrete with the proposed model (Equation 5) of normal concrete, ACI-228.2R,¹⁵ ACI modified linear curve model of normal weight concrete. Similar to the trend observed for a given compressive strength in the case of cylindrical specimens, lightweight concrete shows less pull-out force compared to normal concrete. The study reveals that existing empirical equations available for normal-weight concrete to predict the compressive strength on the basis of pull-out force will not be applicable to lightweight concrete. The developed model will help in predicting the compressive strength of LC-SFA using the pull-out test with a higher degree of accuracy. Figure 16 shows the proposed correlation for lightweight and normal concrete for cube and cylindrical compressive strength. The proposed model for lightweight concrete is compared with the proposed model of normal-weight concrete and the existing ACI-228.2R¹⁵ model for normal concrete. The proposed model for normal concrete is similar and comparable to the ACI model. The difference between the predicted strength value using the pull-out test for both normal and lightweight concrete for a given strength level increases with an increase in compressive strength. The difference in predicted compressive strength value for lightweight concrete by the pull-out test using the developed equation is about 15%–18% higher than the ACI equation and the proposed equation for normal concrete, indicating that for a given pull-out force, lightweight concrete shows more compressive strength compared to normal concrete.

The percentage variation in compressive strength predicted using equations developed by past researchers adopting the pull-out test method and the difference in compressive strength prediction with the developed model are shown in Table 5. The percentage variation in compressive strength predicted by different models varies from -2% to 80% . The model developed by Jensen and ACI for normal concrete gave values somewhat close to the experimental results. However, the variation was more than 15% in the case of ACI, and in the case of

TABLE 5 Existing empirical equations for pull-out test comparison to proposed model.

S. no.	References	Equation (cylinder strength)	Equation (cube strength)	% Variation in compressive strength of LC	Δf_{cy1} (MPa) from 20 to 50 MPa
1	Proposed (LC)	$0.8 \cdot P^{1.12}$	$0.89 \cdot P^{1.16}$	-	-
2	Proposed (NC)	$0.68 \cdot P^{1.12}$	$0.75 \cdot P^{1.16}$	15%–18%	–2 to –6
3	ACI ¹⁵	$0.69 \cdot P^{1.12}$	$0.76 \cdot P^{1.16}$	15%–18%	–2 to –6
4	Manufacture's	$1.25P-6.25$	-	38%–14%	–4) to –5.5
5	Jensen ³¹	$1.12P$	-	–2% to 10%	+0.5 to –4
6	Krenchel ³⁰	-	-	60%–80%	–5.5 to –20

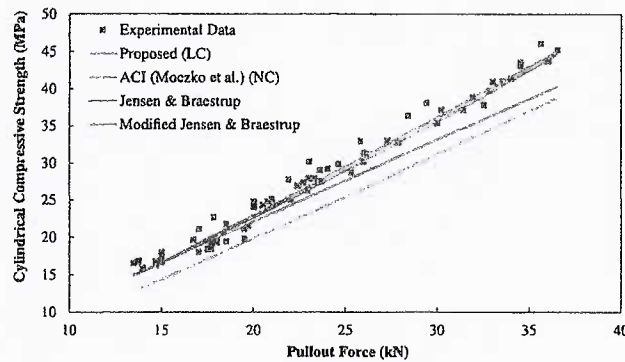


FIGURE 17 Comparison of experimental data, proposed empirical model, and analytical model by Jansen and Braestrup, and modified Jansen and Braestrup model for lightweight concrete.

Jensen, the values were on the lower side. The model reported in the literature for compressive strength prediction of lightweight concrete by Krenchel was also found to be not applicable in the case of LC-SFA. The variation in the predicted compressive values by different models using pull-out force increases as the strength of concrete increases.

6.3 | Comparison of the developed model with analytical models

Few analytical models have been developed in the past to determine compressive strength using the cut and pull-out CAPO test by Jensen and Braestrup,³¹ Bortolotti,³² and Brencich.³⁵ The studies by Li et al.^{36–38} have highlighted that the Jensen and Braestrup equation provides a good fit for test data compared to the Brencich and Mockzko equations. The analytical equation by Jensen and Braestrup indicates that pull-out force variation is directly related to the variation in concrete's compressive strength and failure cone geometry. The theory behind the analytical equation by Jensen and Braestrup assumes concrete between the body of the failure cone to

be rigid, whereas concrete along the conical failure surface is assumed to be plastic. In the analytical model by Jensen and Braestrup, the concrete of the failure cone body was considered rigid, whereas the concrete of the conical failure surface was considered plastic. The Jensen and Braestrup equation, given as Equation (6), has been obtained by equating the rate of internal and external work done through which a pullout force can be obtained.

$$f_{cy} = 2P/S(1 - \sin \phi) \quad (6)$$

In the model by Jensen and Braestrup, the pull-out force is directly correlated to the compressive strength of concrete (f_c) in MPa, the conic shape failure surface area (s) in mm^2 , and the material's angle of internal friction is (ϕ), which is assumed as half of the apex angle. The Bortolotti's compressive strength model was derived considering rigid plastic theory,³⁶ and it was developed under the assumption that the concrete undergoes a hardening process in tension due to the small size of the reaction ring in the apparatus. Bortolotti's equation is shown in Equation (7).³⁹

$$f_c = P/(0.15625 \cdot t \cdot S - 0.0190625 \cdot P) \quad (7)$$

In Bortolotti model, f_c is the concrete's compressive strength (MPa); S is conic shape failure surface area in mm^2 ; P is a pull-out force in N; and t is obtained as ratio of assumed to actual tensile strength. Bortolotti model comes out to be the same as the Jensen and Braestrup model when the angle of internal friction is taken as half of the failure cone apex angle.³⁶

The comparison of experimental data, proposed empirical model for lightweight concrete, and analytical model developed by Jansen and Braestrup for compressive strength determination using cut and pull-out CAPO test has been shown in Figure 17. In Figure 17, the Jansen and Braestrup model has been modified using a

factor determined based on experimental data to predict the compressive strength with more accuracy and reliability for lightweight concrete made with sintered flyash lightweight aggregate.

The modified Equation (8) of the Jansen and Braestrup analytical model can be as follows for prediction of compressive strength of LC-SFA using the cut and pull-out CAPO test method:

$$f_{cy(\text{modified for LC})} = K \times 2P/S(1 - \sin \phi) \quad (8)$$

where K is $(0.005 \times P + 0.925)$ and is the correction coefficient for LC-SFA. The factor K has been developed based on experimental data, which takes into account the material's non-linear behavior, porous microstructure, and bonding characteristics within the matrix of lightweight concrete. The value of K can be modified for the other types of lightweight concrete based on experimental data. The energy required for crack propagation is lower than that of normal concrete, indicating more brittle behavior and through-aggregate failure modes. The relatively weak lightweight aggregate under load causes the propagation of micro-level cracks within ITZ, extending into the aggregate. Whereas in normal-weight concrete, which is strong, it helps in resisting or slowing down the progression of micro-level cracks, with a more controlled failure mode, and is not dominated by direct fracture through the aggregate.

6.4 | Validation of pull-out load results to stress-strain parameters of concrete

The stress-strain curve for concrete with LC-SFA and normal concrete is shown in Figure 18. When comparing the stress-strain behavior of normal and lightweight concrete, it is observed that the ascending branch of normal concrete remains linear up to 45%–50% of the peak load, but in the case of lightweight concrete, it exhibits a higher degree of linearity, extending to approximately 80% to 85% of the peak load. The descending stage of LC-SFA is steeper than that of normal concrete, especially for higher strength levels above 25 MPa, indicating greater brittleness.

In Figure 19a, the plot of the ratio of ultimate strain (ϵ_u) to strain at peak stress (ϵ_o) corresponding to peak stress has been shown for concrete with sintered flyash lightweight coarse aggregate and normal weight concrete. Figure 19b presents the developed trend line of the ratio of ultimate strain to strain at peak stress vs. peak stress for normal and lightweight concrete. The results presented in Figure 19, indicate that with an increase in

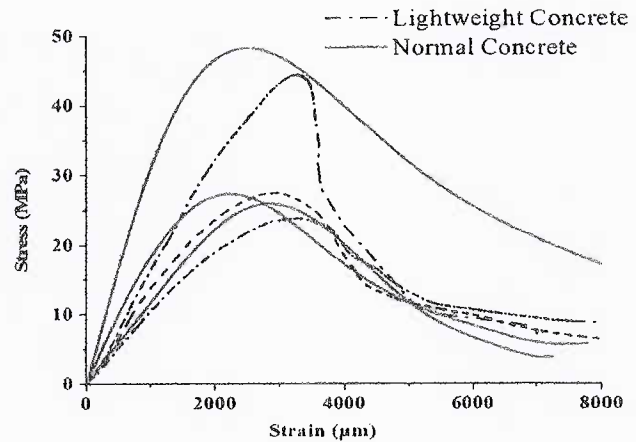


FIGURE 18 Stress-strain curve for normal concrete (NC) and light-weight concrete (LC).

compressive strength of concrete, the ϵ_u/ϵ_o decreases for both lightweight and normal weight concrete. The ascending linear part of the stress-strain curve represents the elastic behavior and reflects the overall stiffness of the LC-SFA. The stiffness is primarily impacted by the aggregate-paste matrix bond quality. The cut and pull-out test quantifies the parameters related to the pull-out test, such as initial bond strength and resistance to interfacial separation of concrete. The impact of the bond is related to the modulus of elasticity and the initiation of cracking. The early linear part of the stress-strain curve is related to the effective bonding property assessed through the cut and pull-out test. The surface characteristics of lightweight aggregate, along with its porous nature and internal curing effects in lightweight concrete, contribute to a more refined and enhanced ITZ. This results in the formation of a monolithic ITZ, ultimately extending the ascending branch of the compressive stress-strain curve. In lightweight concrete, failure occurs in a brittle manner once a fracture is initiated due to a weaker aggregate interlocking mechanism, causing cracks to propagate through the aggregates.^{40–43} In contrast, normal concrete experiences fracture initiation at the aggregate-mortar interface, with cracks propagating around the aggregates. The pull-out test captures the localized failure, such as micro-level cracking and pull-out phenomena at the aggregate paste interface. The pull-out test helps to interpret the softening and brittle behavior, which may appear as the stress-strain curve reaches peak strength and drops sharply after reaching peaks. The sintered flyash lightweight aggregate, due to its typical microstructure, compared to normal concrete, shows a longer linear response and a steeper descending branch, addressing the heterogeneity in the materials at the micro-scale, ultimately influencing macro-scale failure in the pull-out

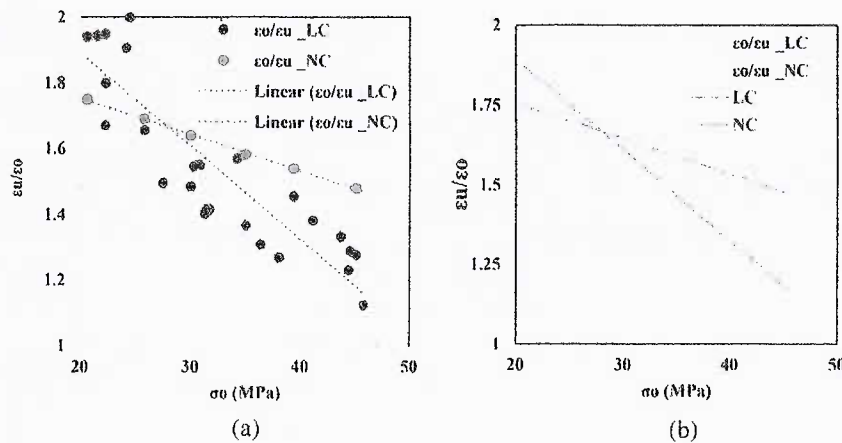


FIGURE 19 (a) Ratio of ultimate strain to strain at peak stress vs. compressive stress for normal and lightweight concrete. (b) Trend line of ratio of ultimate strain to strain at peak stress vs. compressive stress for normal and lightweight concrete.

TABLE 6 Comparison of compressive strength from developed model using cut and pull-out test and concrete core test for lightweight concrete made with sintered flyash lightweight aggregate.

S. no.	Concrete core strength of 100 mm diameter (MPa)	Cut and pull-out force (kN)	Cylindrical compressive strength using developed model for cut and pull-out	Relative error (core strength – pull-out)/Core strength
1	21.25	19.60	22.40	5.41
2	20.75	17.25	19.42	6.40
3	23.95	21.55	24.92	4.40
4	35.05	33.97	41.50	18.40
5	33.76	32.69	39.75	17.74
6	38.43	36.23	44.60	22.42

test. The lower intrinsic modulus of concrete with sintered flyash lightweight aggregate iterates the fact that the bond between paste and aggregate for lightweight concrete is lower than that for normal weight concrete, and also, aggregate interlock is minimal, resulting in lower pull-out force.

The lightweight concrete generally exhibits through-aggregate type fracture on the conical failure than normal weight concrete, due to the intrinsic properties and microstructure of the aggregate. Under the pull-out load, the weak aggregates allow propagation of cracks directly through and through rather than deflecting or inhibiting at the boundary of the aggregate, leading to through-aggregate fractures on the failure plane. The low level of fracture energy and diminished crack-arresting behavior of sintered flyash lightweight aggregate indicate that after initiation of a crack, there is an easy pathway for crack propagation through the aggregate. The above-mentioned factors highlight that concrete made with sintered flyash lightweight aggregate shows brittle conic failure with pronounced through-aggregate fractures, where the aggregate does not provide a barrier to the propagation of

the crack into the aggregate, influencing the failure under pull-out stresses.

6.5 | Verification of the developed pull-out model with concrete core test results

The reliability and accuracy of the developed empirical model for determining compressive strength of lightweight concrete using the cut and pull-out test have been checked through a limited number of concrete core samples extracted from a three-year-old concrete beam cast with lightweight aggregate at laboratory scale. The results are given in Table 6. The concrete core of 100 mm diameter was extracted from the concrete beams, and on the same beams cut and pull-out test was performed. The height-to-diameter ratio of concrete cores was nearly kept constant in the range of 1.05–1.10. A total of six concrete cores have been taken from two concrete mixes having a w/c ratio of 0.6 and 0.4 (as shown in Table 3, panel a), with 28-day cube compressive strengths of 23.66 and 43.37, respectively. The concrete cores were extracted

from each of the two mixes mentioned above. The average of three concrete cores tested in compression represents effective data for each mix. The concrete cores are properly cut and ground for applying uniform loading. For the concrete core diameter of 100 mm and aspect ratio (length to diameter of core between 1.05–1.10), it can be assumed that concrete core strength is equivalent to the compressive strength of a 150 mm cube of the same concrete strength as per EN-13791.^{14,44}

The relative error between the core strength and the cut and pull-out strength obtained using the developed model varies between 4.40 and 5.41 for lightweight concrete having a w/c ratio of 0.6 (Table 6). The relative error between the core strength and the cut and pull-out strength obtained using the developed model varies between 17.74 and 22.42 for lightweight concrete having a w/c ratio of 0.4 (Table 6). The results indicate that the cut and pull-out method overestimates the compressive strength significantly compared to concrete core test results for lightweight concrete grades having strength above 30 MPa, as seen from the cut and pull-out results. These findings are similar to the study done by Yang et al.¹⁴ using the modified pull-out test method for on-site strength determination. In the present study, only limited concrete core samples could be extracted for verification of the developed model for lightweight concrete with sintered flyash lightweight aggregate. However, the developed model can be further calibrated through the accumulation of field data. The cut and pull-out test directly depends upon the measurement of pull-out force, and the pull-out force is snapshot to the current strength of concrete. The current strength of on-site concrete, depending upon the mix composition, gets influenced by ongoing hydration, environmental conditions such as the curing regime, and changes in the microstructure of concrete over time. The consideration of long-term strength development law becomes critical when test is conducted at longer ages and environmental conditions are different than the standard. The developed model for lightweight concrete using sintered flyash lightweight aggregate in the present study does not account for predicted strength gain over time.

7 | CONCLUSIONS

The objective of the present study was to assess the applicability of the existing models which has been established earlier for normal concrete for predicting on-site compressive strength of lightweight concrete made using sintered flyash lightweight coarse aggregate using the pull-out method. Additionally, the study also aimed to develop a new correlation between the pull-out force and

compressive strength of concrete for both cylindrical and cube compressive strength when sintered flyash lightweight aggregate is used as the coarse aggregate. Based on the study conducted, the following conclusions are drawn:

- The pull-out method adopted in the study has demonstrated that the in-place compressive strength of concrete can be predicted with high accuracy and better repeatability of concrete made using sintered flyash lightweight coarse aggregate.
- The test results indicate that for a given compressive strength, lightweight concrete shows less pull-out force as compared to normal-weight concrete. The reduction in pull-out force for lightweight concrete for a given strength level is mainly due to the absence of aggregate interlock contribution to the failure mechanism. The lightweight concrete generally exhibits through-aggregate type fracture on the conical failure than normal weight concrete, due to the intrinsic properties and microstructure of the aggregate. Under the pull-out load, the weak aggregates allow propagation of cracks directly through and through rather than deflecting or inhibiting at the boundary of the aggregate, leading to through-aggregate fractures on the failure plane.
- In the pull-out test, the failure mode consists of vertebral and vertebral-bond composite failure. The test surface characteristics have a very small influence on the failure modes under the pull-out test, and the most common mode of failure noted is vertebral failure.
- The proposed model for sintered fly ash aggregate-based lightweight concrete has been compared with various established models, mainly for normal-weight concrete. These included the manufacturer's curve, the ACI-228 model, and the Jensen et al. models for normal-weight concrete, as well as the Krenchel et al. model for lightweight concrete. The percentage variation in compressive strength predicted by different models varies from –2% to 80%. The model developed by Jensen and ACI for normal concrete gave values somewhat near to the experimental results; however, the variation was more than 15% in the case of ACI, and in the case of Jensen, the values were on the lower side.
- The lower intrinsic modulus of concrete with sintered flyash lightweight aggregate, as evident from stress-strain behavior, iterates the fact that the bond between paste and aggregate for lightweight concrete is lower than normal weight concrete, and also, aggregate interlock is minimum, resulting in lower pull-out force. The impact of the bond is related to the modulus of

elasticity and initiation of cracking. The early linear part of the stress-strain curve is related to the effective bonding property assessed through the cut and pull-out test. The surface characteristics of lightweight aggregate, along with its porous nature and internal curing effects in lightweight concrete, contribute to a more refined and enhanced ITZ.

- The study revealed that existing empirical equations available for normal-weight concrete to predict the compressive strength based on pull-out force will not apply to lightweight concrete. For high accuracy and repeatability, the proposed model for the prediction of cylindrical compressive strength and cube compressive strength of sintered flyash lightweight aggregate-based concrete is $f_{cy} = 0.8 \cdot P^{1.12}$ and $f_c = 0.89 \cdot P^{1.16}$, respectively.
- The Jansen and Braestrup analytical model can be modified as $f_{cy(\text{modified for LC})} = K \times 2P/S (1 - \sin \phi)$ for prediction of compressive strength of lightweight concrete using the cut and pull-out CAPO test method, where K is $(0.005 \times P + 0.925)$ and is the correction coefficient for lightweight concrete made with sintered flyash lightweight aggregate.


CONFLICT OF INTEREST STATEMENT


The authors declare no conflicts of interest.


DATA AVAILABILITY STATEMENT

The data that support the findings of this study are available from the corresponding author upon reasonable request.


ORCID

Brijesh Singh  <https://orcid.org/0000-0002-6512-1968>

Shamsher Bahadur Singh  <https://orcid.org/0000-0001-6847-0701>

Sudhirkumar V. Barai  <https://orcid.org/0000-0001-5100-0607>

P. N. Ojha  <https://orcid.org/0000-0003-1754-4488>

Rohit Kumar  <https://orcid.org/0009-0000-6167-375X>

REFERENCES

1. Singh B, Singh SB, Barai SV. Performance of concrete made using sintered flyash lightweight aggregate-a review. *Indian Concr J*. 2023;97(7):41–59.
2. Ojha PN, Singh B, Behera AK. Sintered flyash lightweight aggregate-its properties and performance in structural concrete. *Indian Concr J*. 2021;95(6):20–30.
3. Nadesan MS, Dinakar P. Structural concrete using sintered flyash lightweight aggregate: a review. *Construct Build Mater*. 2017;154:928–44.
4. Skramtajew BG. Determining concrete strength for control of concrete in structures. *ACI Mater J*. 1938;34(3):205–304.
5. Rutenbeck T. New developments in in-place testing of shotcrete. Use of shotcrete for underground structural support. Report no. SP-45. Detroit: American Concrete Institute; 1974. p. 246–62.
6. Kierkegaard P. Lok-strength. *Nordish Betong*. 1975;19(3):19–28.
7. Malhotra VM. Evaluation of the pull-out test to determine the strength of on-site concrete. *Mater Struct*. 1975;8(43):19–31.
8. Richards O. Pull-out strength of concrete reproducibility and accuracy of mechanical tests. ASTM STP Rep. no. 626. Philadelphia, PA: American Society for Testing and Materials; 1977. p. 32–40.
9. Stone WC, Carino NJ. Deformation and failure in large-scale pull-out tests. *ACI Mater J*. 1983;80(6):501–13.
10. Collins FG, Roper H. Evaluation of concrete spall repairs by pull-out test. *Mater Struct*. 1989;22:280–6.
11. Yang S, Hu C, Xu Z. Experimental study on compressive strength of in situ concrete tested with arc pressure method. *Mag Concr Res*. 2024;76(9):427–37.
12. Yang S, Zhu H, Xu Z. Prediction of compressive strength of concrete using double-shear testing method. *J Mater Civ Eng*. 2021;33(1):04020423.
13. Yang S, Gao G, Xu Z. Estimation of in situ masonry mortar compressive strength using hammer pendulum test method. *Mag Concr Res*. 2025;77:722–31. <https://doi.org/10.1680/jmacr.24.00416>
14. Yang S, Xu Z, Bian Z. Prediction on compressive strength of concrete using modified pull-off testing method (MPTM). *Construct Build Mater*. 2020;250:118834. <https://doi.org/10.1016/j.conbuildmat.2020.118834>
15. ACI Committee 228. ACI 228.2R-13: in-place methods to estimate concrete strength. Farmington Hills: American Concrete Institute; 2013.
16. Pannuzzo P, Tutton M, Furlan M, Tecchio G. Evaluation of the pull-out test to determine the residual prestressing in concrete bridges. *CE/Papers*. 2023;6(5):53–9.
17. IS: 9142 (Part-2). Artificial lightweight aggregate for concrete-specification, Part 2—Sintered flyash coarse aggregate. Delhi: BIS; 2018.
18. Singh B, Singh SB, Barai SK, Ojha PN. A simplified mix proportioning method for structural grade lightweight concrete using sintered flyash lightweight aggregate. International conference on sustainable materials, environment & technologies under climate change scenario (SMEET-2024). Haryana: NIT Kurukshetra; 2024.
19. Arora VV, Singh B, Patel V, Trivedi A. Evaluation of modulus of elasticity for normal and high-strength concrete with granite and calc-granulite aggregate. *Struct Concr*. 2021;22(S1):E143–51.
20. Ojha PN, Singh B, Singh P, Singh A, Mittal P. Experimental determination of stress-strain characteristics of very high strength unconfined concrete in compression including comparison with normal and high strength concrete. *Revista Ingeniería de Construcción RIC, Chilee*. 2023;37(3):25–39.
21. IS: 10262. Concrete mix proportioning-guidelines. Delhi: BIS; 2019.
22. IS: 516 (Part 1/Sec 1). Hardened concrete-methods of test part-1, testing of strength of hardened concrete, section-1: compressive, flexural, and split tensile strength. Delhi: BIS; 2021.

23. ASTM C-900. Standard test method for pullout strength of hardened concrete. ASTM standards. West Conshohocken, PA: ASTM International; 2023.
24. British Standard BS. 1881-207: testing concrete—recommendations for the assessment of concrete strength by near-surface tests. London: BSI; 1999.
25. European Standard EN 12504-3. Testing concrete in structures—part 3: determination of pull-out force. European committee for standardization (CEN). Belgium: Comité Européen de Normalisation; 2005.
26. RILEM Technical Committee 207-INR. Non-destructive assessment of concrete structures: reliability and limits of single and combined techniques: state-of-the-art report. The Netherlands: Springer Science & Business Media; 2012.
27. Nasrin US, Khair A, Ahsan R. Compressive strength assessment of concrete with brick chips using the CAPO-test. *Sci Rep*. 2024;14(1):12881.
28. Krenchel H. Lok-strength and capo-strength of concrete, ABK Publication, Series I. Vol 71. Lyngby: Structural Research Laboratory, Technical University of Denmark; 1982.
29. Krenchel H, Bickley JA. Pull-out testing of concrete—historical background and scientific level today. Vol 6. Norway: Nordic Concrete Federation; 1987.
30. Krenchel H, Shah SP. Fracture analysis of the pull-out test. *Mater Struct*. 1985;18(108):439–46.
31. Jensen BC, Braestrup MW. Lok-test determine the compressive strength of concrete. *Nordisk Betong*. 1976;2:9–11.
32. Bortolotti L. Strength of concrete subjected to pull-out load. *J Mater Civil Eng*. 2003;15(5):491–5.
33. Li J, Ren X. Stochastic damage model for concrete based on energy equivalent strain. *Int J Solids Struct*. 2009;46(11–12):2407–19.
34. Mazars J. A description of micro-and macroscale damage of concrete structures. *Eng Fract Mech*. 1986;25(5–6):729–37.
35. Brencich A. A post-installed insert for pull-out tests on concrete up to 70 MPa. *Construct Build Mater*. 2015;95:788–801.
36. Li Z. A new method of estimating equivalent specified compressive strength of existing concrete based on probabilistic modeling of pull-out test. *J Build Rehabil*. 2022;7(73):1–11. <https://doi.org/10.1007/s41024-022-00217-7>
37. Li Z, Desai J, Bullock W. In-place estimation of concrete compressive strength using post-installed pullout test—a case study. *J Test Eval*. 2020;48:1319–33.
38. Li Z, Desai J. Investigative assessment of concrete slab using non-destructive evaluation techniques. *Structures congress*. Reston VA: American Society of Civil Engineers; 2019. p. 162–70.
39. Bortolotti L. Punching shear strength in slabs. *ACI Struct J*. 1990;87(2):208–19.
40. Simo JC, Ju JW. Strain-stress based continuum damage models—I formulation. *Math Comput Model*. 1989;12(3):378–90.
41. Singh B, Arora VV, Patel V. Experimental study on stress-strain behaviour of normal and high strength unconfined concrete. *Indian Concr J*. 2020;94(4):10–9.
42. Singh B, Singh SB, Barai SV, Ojha PN, Kumar R. Fracture behavior of concrete made with sintered flyash lightweight coarse aggregate in comparison to normal weight concrete. *J Res Eng Struct Mater*. 2024;11(2):761–81. <https://doi.org/10.17515/resm2024.310me0607rs>
43. Singh B, Singh SB, Barai SV, Ojha PN, Kumar R. Mechanical properties and fracture behavior of concrete made with sintered flyash lightweight coarse aggregate and electric arc furnace slag as fine aggregate. *J Res Eng Struct Mater*. 2024. <https://doi.org/10.17515/resm2024.396me0814rs>
44. BS EN 13791. Assessment of on-site compressive strength in structures and pre-cast concrete components. Belgium: Comité Européen de Normalisation; 2007.

AUTHOR BIOGRAPHIES



Brijesh Singh is a PhD Research Scholar at Birla Institute of Technology and Science (BITS) Pilani, Rajasthan, India and a General Manager in Centre for Construction Development and Research in National Council for Cement and Building Materials, Ballabgarh, Haryana, India. Email: brijesh.singh@ncbindia.com



Shamsher Bahadur Singh is a Senior Professor in the Department of Civil Engineering and Dean (Infrastructure and Planning) at Birla Institute of Technology and Science (BITS) Pilani, Rajasthan, India. Email: sbsinghbits@gmail.com



Sudhirkumar V. Barai, is a Senior Professor in the Department of Civil Engineering and Director at Birla Institute of Technology and Science (BITS) Pilani, Rajasthan, India. Email: skbarai@pilani.bits-pilani.ac.in



P. N. Ojha, is a Joint Director in the Centre for Construction Development and Research in National Council for Cement and Building Materials, Ballabgarh, Haryana, India. Email: pnojhaji@gmail.com



Rohit Kumar, is a Deputy Manager in the Centre for Construction Development and Research in National Council for Cement and Building Materials, Ballabhgarh, Haryana, India.
Email: rohitkmr771@gmail.com

How to cite this article: Singh B, Singh SB, Barai SV, Ojha PN, Kumar R. Empirical model for determining compressive strength using post-installed pull-out test for structural lightweight concrete made with sintered flyash lightweight aggregate. *Structural Concrete*. 2025. <https://doi.org/10.1002/suco.70219>